Automated Liver Tumor Segmentation and Staging Method Using 3D U-Net in CT Images*

Soohyun Kim
Department of Computer Science and Engineering
Soongsil University
Korea
sooo0426@soongsil.ac.kr

Dayoung Hwang
Department of Computer Science and Engineering
Soongsil University
Korea
qbddjehd@naver.com

Sunyoung Lee
Department of Radiology and Research Institute of Radiological Science
Severance Hospital, Yonsei University College of Medicine
Korea
carnival0126@gmail.com

Jeongjin Lee
School of Computer Science and Engineering
Soongsil University
Korea
leejeongjin@ssu.ac.kr

ABSTRACT

Accurate [1] diagnosis and staging of Hepatocellular Carcinoma (HCC) are essential for formulating treatment strategies and assessing patient prognosis. Diagnosis and staging of HCC necessitate the review of hundreds of Computed Tomography (CT) images to identify lesions. The process is time-consuming and relies heavily on the subjective judgment of medical professionals, thereby introducing the risk of misdiagnosis. This paper proposes an automatic liver tumor segmentation and staging method to address the issues and to achieve objective and accurate diagnosis and staging of HCC. The proposed method utilizes a 3D U-Net to automatically segment the liver, liver vessels, and tumor regions from CT images, subsequently generating a surface mesh of the segmented areas. From this generated mesh, the number, size, and vascular invasion of tumors are assessed, and staging is conducted based on these parameters. The accuracy of the proposed method is evaluated through experiments. The experimental results demonstrate that the proposed method can accurately stage HCC, contributing to the objective and precise diagnosis and staging of HCC.

RACS '24, November 5–8, 2024, Pompei, Italy

ACM ISBN 979-8-4007-0606-6/24/11…
https://doi.org/10.1145/3649601.3698741

CCS CONCEPTS

• **Computing methodologies** → **Computer graphics** → **Image manipulation** → Image processing;

KEYWORDS

Medical imaging, CT Image, Segmentation, Deep Learning, Hepatocellular carcinoma, Tumor Staging

ACM Reference format:

S. Kim, D. Hwang, S. Lee and J. Lee. 2024. Automated Liver Tumor Segmentation and Staging Method Using 3D U-Net in CT Images. In *Proceedings of ACM RACS Conference, Pompei, Italy, November 5 – November 8, 2024 (RACS'24),* 7 pages. DOI: https://doi.org/10.1145/3649601.3698741

1 INTRODUCTION

In Primary liver cancer is one of the most common malignant tumors. According to the 2021 World Cancer Data Report, primary liver cancer ranks as the seventh most frequently cancer globally and is the second leading cause of cancer-related deaths[1]. HCC, a malignant tumor originating from hepatocytes, accounts for approximately 90% of primary liver cancers.

HCC can be effectively treated with simple resection surgery if diagnosed at an early stage. However, more advanced cases require chemotherapy, and in the worst scenarios, treatment may be infeasible[2]. The prognosis varies significantly with the stage of the disease; the five-year survival rate for advanced HCC is approximately 20%, while it is about 70% for early-stage HCC. Accurate diagnosis and staging of HCC are crucial for developing effective treatment plans and predicting long-term patient outcomes[3].

Due to the highly vascularized nature of the liver, which increases the risk of tumor seeding and bleeding, radiological modalities such as CT and MRI are preferred for diagnosing HCC over tissue biopsies[4]. The diagnosis and staging of HCC involve a labor-intensive process in which clinicians visually assess hundreds of CT images. This process is time-consuming and relies on subjective judgment, leading to the potential risk of misdiagnosis.

Several related studies have been conducted in this area. Manjunath et al[5]. utilized a Modified ResUnet to automatically segment the liver and liver tumors. While the segmentation performance was high, with a DSC of approximately 96.3 for the liver and 89.2 for liver tumors, the method had limitations due to the conversion of 3D data into a 2D format for training, leading to risk of information loss, and it could not segment vessels.

Kavitha et al[6]. used histopathological images of early, intermediate, and late-stage liver cancer to automatically classify liver cancer stages using an R-CNN model. The proposed model achieved a high classification accuracy of 96.7%; however, the need for biopsy to obtain data introduces risks of bleeding and tumor seeding.

Xu et al[7]. utilized a Swin-Transformer to determine the LI-RADS grade of tumors and differentiate HCC from non-HCC using multi-phase CT images. Their model efficiently determined LI-RADS grades with accuracy comparable to that of radiologists. Midya et al[8]. used semi-automatically segmented tumor images from CT scans to train a deep learning model based on the Inception v3 network, differentiating HCC, ICC, colorectal liver metastasis (CRLM), and benign tumors with high accuracy. However, both studies did not address the staging of HCC.

In this paper, we propose an automatic liver tumor segmentation and staging technique using CT images to address these limitations. The proposed method is structured as follows: first, appropriate preprocessing steps are applied to generate data suitable for training. Next, a 3D U-Net[9] is employed to segment the liver, liver vessels, and tumors, and to generate surface meshes of the segmented regions. Finally, the staging of HCC is determined based on the generated surface meshes.

The rest of this paper is as follows. Section 2 explains the liver tumor segmentation and staging method. Section 3 presents the experimental setup, and experimental results. Finally, Section 4 concludes the paper.

2 METHODS

This paper proposes an automatic liver tumor segmentation and staging technique utilizing a 3D U-Net. The proposed method follows the process outlined in Figure 1.

Initially, preprocessing and data augmentation are performed on the training data. Next, a 3D U-Net is used to train models for segmenting the liver region, liver vessel region, and tumor region. The trained models are then applied to segment the liver, liver vessels, and liver tumor regions, and to generate surface meshes of the segmented areas. Finally, the generated surface meshes are used to determine the number, size, and vascular invasion of the tumors, which are then used to classify the staging of HCC.

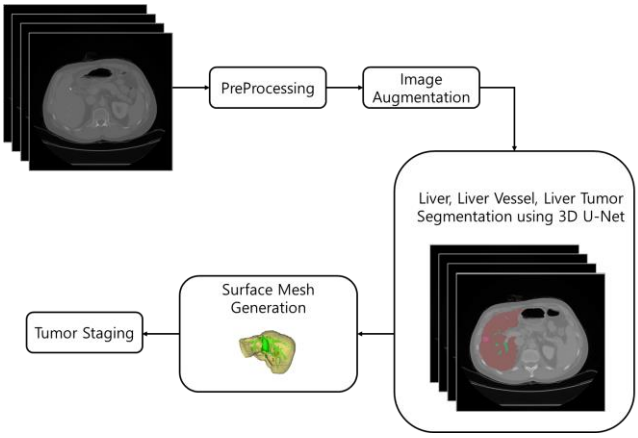

Figure 1: Liver Tumor Segmentation and Staging process

2.1 Data Set

This paper applies two datasets. The first dataset is used for training the proposed model, while the second dataset is used to evaluate the accuracy of the staging method for HCC.

2.1.1 Training Dataset. For model training, the Hepatic Vessel dataset provided by Decathlon is used[10]. This dataset consists of 443 portal-venous phase CT images obtained from patients with various primary and metastatic liver tumors (including cholangiocarcinoma, hepatocellular carcinoma, and metastatic liver cancer). The primary regions of interest (ROI) in each image are the liver vessels and tumors. Each image has a resolution of 512 x 512 pixels, with varying numbers of slices per patient.

2.1.2 Experimental Dataset. For staging hepatocellular carcinoma (HCC), the HCC-TACE-Seg dataset provided by TCIA is used[11]. This dataset comprises CT images from 105 patients with HCC and includes TNM staging information. Each image has a resolution of 512 x 512 pixels, with varying numbers of slices per patient. 20 cases from this dataset are used to assess the accuracy of the staging method.

2.2 Data Preparation

2.2.1 Data Generation for Training. The training dataset is generated using TotalSegmentator[12], a model based on nnU-Net[13]. While TotalSegmentator can segment 117 organs and tissues, including the heart, lungs, liver, and kidneys, it does not support the segmentation of liver vessels and liver tumors. For training a model that can segment the liver, liver vessels, and liver tumors, the liver region is segmented using TotalSegmentator on the training dataset from the Decathlon dataset. The segmented regions are then integrated with the existing labels from the dataset, resulting in new labels: 1 for liver, 2 for hepatic vessels, and 3 for liver tumors. This process generates a new dataset for training. Figure 2 shows the process of generating the new training data. (a) is the original CT image, (b) shows the segmentation results of the liver region, and (c) depicts the result of integrating the liver region into the existing labels.

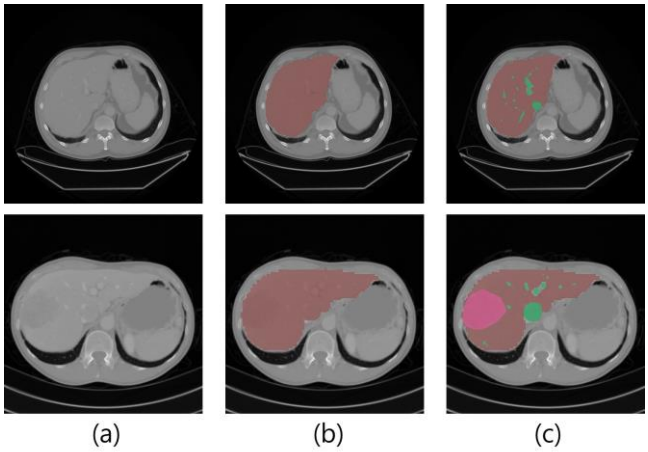

Figure 2: Process of generating the training data: (a) original CT image, (b) liver region segmentation result, (c) result of integrating the liver region into the existing labels.

2.2.2 Data Augmentation. To enhance the model's generalization performance and prevent overfitting, data augmentation is employed. Data augmentation is a techniques that artificially increases the amount of data through computer algorithms based on a limited dataset, addressing issues of data scarcity and imbalance.

In this paper, augmentation techniques are applied randomly to ensure a balanced inclusion of positive and negative samples. Techniques include CropByPosNegLabeld to balance sample types, Flip to perform axis inversion with a 50% probability along each spatial axis, Rotate to rotate images in multiples of 90 degrees, Zoom to randomly scale images by a factor between 0.9 and 1.1 with a 20% probability, ShiftIntensity to randomly alter pixel values by 0.1 with a 50% probability, and Affine to apply rotation, scaling, and translation transformations with a 50% probability.

2.2.3 Data Preprocessing. Finally, preprocessing is performed to adapt the data for model training. Effective preprocessing is crucial, as it directly influences the performance of deep learning models.

Initially, pixel values in the CT images are normalized to a range of -140 HU to 260 HU, which corresponds to the liver's density range. This is followed by linear scaling to a range of 0.0 to 1.0 to convert the data into a suitable input format for model training. Subsequently, foreground detection is performed on the images and labels to crop out unnecessary background. The cropped images and labels are resized to uniform dimensions, using bilinear interpolation for images and nearest-neighbor interpolation for labels to enhance consistency in model training and effectively handle data with varying resolutions. Next, an Anisotropic Diffusion Filter (ADF)[14] is applied to the input images to remove noise while preserving the boundaries of the liver and vessels. Finally, histogram equalization is employed to improve the image contrast and uniformly distribute brightness values, enhancing the visibility of image details. Figure 3 shows the results of the preprocessing.

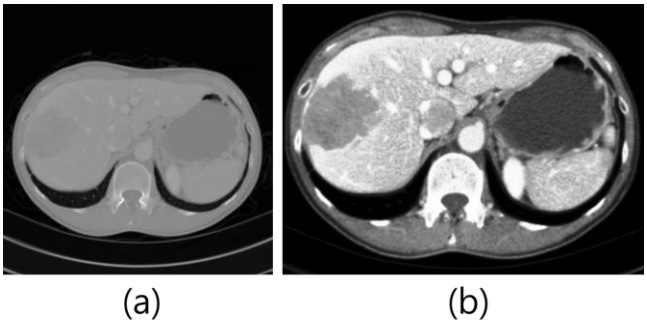

Figure 3: Image preprocessing: (a) abdominal CT image before preprocessing, (b) image preprocessing result.

2.3 Deep Learning Segmentation

A deep learning model is trained to automatically segment the liver, liver vessels, and liver tumors using a 3D U-Net. The 3D U-Net extends the 2D U-Net architecture to three dimensions, optimizing it for processing 3D volumetric data. This deep learning model demonstrates high performance through an effective encoder-decoder architecture. Figure 4 shows the network architecture of the 3D U-Net.

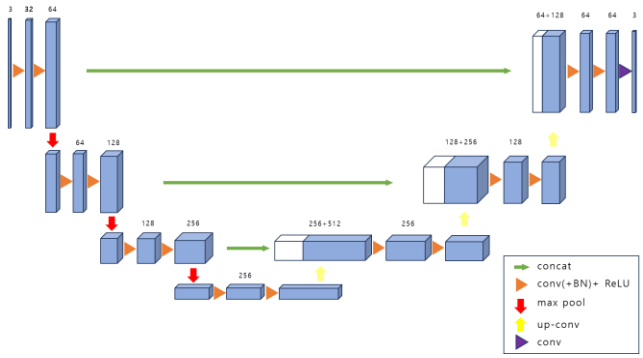

Figure 4: Network architecture of the 3D U-Net.

The 3D U-Net model features a symmetric U-shaped structure composed of encoder and decoder blocks. Each encoder block consists of 3D convolution, ReLU activation functions, and 3D max pooling layers. These encoder blocks progressively reduce the spatial resolution of the input images while extracting essential features. The decoder blocks use 3D up-convolution along with incorporate skip connections to combine features extracted by the encoder. This process produces higher-resolution outputs and enhances segmentation performance. Skip connections link corresponding layers between the encoder and decoder, facilitating the transfer of low-level spatial information from the encoder to the decoder. This mechanism enables the network to preserve detailed spatial information even in deeper

layers. Due to these structural characteristics, the model achieves high accuracy with a relatively small number of parameters and effectively segments lesions of various sizes.

The Adam optimizer is employed to optimize the network weights with a learning rate of $1e-4$, minimizing the Dice loss function to train the model parameters. The learning rate is initially set to 0.001 and is subsequently decreased as training progresses. Figure 5 shows the training results.

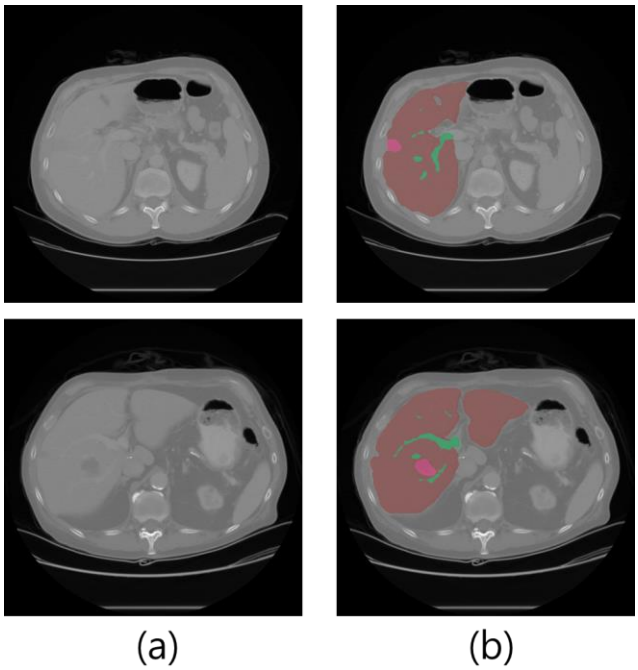

Figure 5: Training result: (a) before segmentation, (d) after segmentation.

The segmented liver, liver vessels, and liver tumors regions are used to generate surface meshes for the liver, liver vessels, and liver tumors. The mesh generation is accomplished using the Flying Edges[15] method. The Flying Edges algorithm is a method for extracting contours from 3D volumetric data, operating both rapidly and efficiently. The algorithm operates as follows.

First, it is determined whether the contour intersects each edge. This is checked by examining if the values at the two endpoints of the edge, v_1 and v_2, cross the threshold value v_t. The condition for this is:

$$(v_1 - v_2) \cdot (v_2 - v_t) < 0 \quad (1)$$

If this condition is satisfied, an intersection occurs on the edge. The exact position of the intersection is then calculated using linear interpolation:

$$P = P_1 + \frac{v_t - v_1}{v_2 - v_1}(P_2 - P_1) \quad (2)$$

Where P denotes the position of the intersection, and P_1 and P_2 are the positions of the two endpoints of the edge. Finally, the intersections are computed along the edges of each cell. Each cell represents a small portion of the 3D volumetric data. By identifying intersections along each edge of the cell and connecting them, the contour is generated.

The surface mesh of the segmented regions is constructed through this process. Figure 6 shows the surface mesh produced using this method.

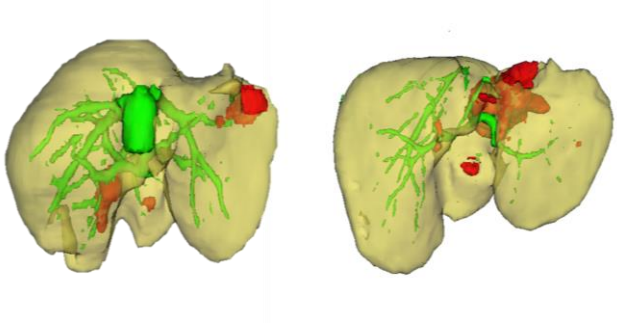

Figure 6: Constructed surface mesh.

2.4 Staging

The staging is performed using the surface meshes generated in Section 2.3. The staging is conducted using the TNM system developed by the UICC[16]. The TNM staging system is shown in Table 1.

Table 1: TNM staging system

Staging (AJCC 8th)	N0	N1	M1
T1	Stage I	Stage III	Stage IV
T2			
T3	Stage II		
T4			

Initially, the T stage determines the size and extent of tumor invasion. T1 is assigned for a single tumor measuring 2cm or less with no vascular invasion. T2 indicates a single tumor exceeding 2cm with mild vascular invasion or multiple tumors, all 5cm or less in diameter. T3 is designated for multiple tumors, with at least one exceeding 5 cm. T4 is assigned when there is invasion of the major branches of the hepatic portal vein or hepatic vein, regardless of tumor size or number. Subsequently, the N stage evaluates lymph node metastasis. N0 indicates no metastasis to nearby lymph nodes, while N1 signifies metastasis in adjacent lymph nodes. Finally, the M stage identifies metastasis to other organs. M0 indicates no spread to other sites, whereas M1 denotes metastasis outside the liver. Other staging classification systems,

aside from TNM, additionally consider factors such as serum albumin levels and liver function to determine the stages.

In this paper, staging is performed solely using abdominal CT images, which precludes the application of established staging systems such as TNM. Consequently, the TNM system is applied for staging as follows: Stage 1 is assigned for a single tumor with a diameter of 2cm or less. Stage 2 is assigned if there is a single tumor with a diameter between 2cm and 5cm, or if there are multiple tumors, each with a diameter of 5cm or less. Stage 3 is assigned when there are multiple tumors and at least one tumor has a diameter greater than 5cm. Stage 4 is designated if there is invasion of the major branches of the hepatic portal vein or hepatic vein, regardless of the tumor size or number, due to the high likelihood of metastasis through the blood vessels to other surrounding organs. Vessels with a diameter of 5mm or more are considered major branches of the hepatic portal vein or hepatic vein.

Algorithm 1 Tumor Staging Algorithm

Input: Liver Surface mesh L, Liver Vessel Surface mesh V, Liver Tumor Surface mesh T
Output: Predicted Stage S

for each t_i in T;
  for each c_i in InvasionPoint(t_i, V);
    if vessel_diameter(c_i) >= 5;
      $S = 4$;
    end if;
  end for;
  if tumor_diameter(t_i) >= 50;
    $S = 3$;
  else if tumor_diameter(t_i) < 20;
    $Tumor$ += 1;
  end if;
end for;
if S == 0 and $Tumor$ == 1;
  $S = 1$
else if S == 0;
  $S = 2$
end if
return S

The staging algorithm operates as described in Algorithm 1. First, the diameter of each tumor t_i in the Tumor Surface Mesh T is assessed. Next, all intersection points c_i where t_i intersects with the Vessel Surface Mesh V are identified. If the diameter of the vessel at c_i is 5mm or greater, Stage 4 is assigned. Tumors with a diameter of 5cm or more are classified as Stage 3, single tumors with a diameter less than 2cm are classified as Stage 1, and all other cases are classified as Stage 2.

3 EXPERIMENTAL RESULTS AND EVALUATIONS

The evaluation consists of both qualitative and quantitative assessments. Initially, qualitative evaluation is conducted to visually demonstrate the performance of the segmentation model. This is followed by quantitative evaluation, which measures the accuracy of the segmentation model and the precision of the staging classification.

3.1 Qualitative Evaluation

Figure 7 shows the segmentation results. (a) shows the original CT image, (b) presents the segmentation results, (c) shows the original ground truths segmentation regions, and (d) shows the overlay of the segmentation results on the original CT image. The proposed method visually demonstrates the high accuracy in segmenting the liver, liver vessels, and liver tumors.

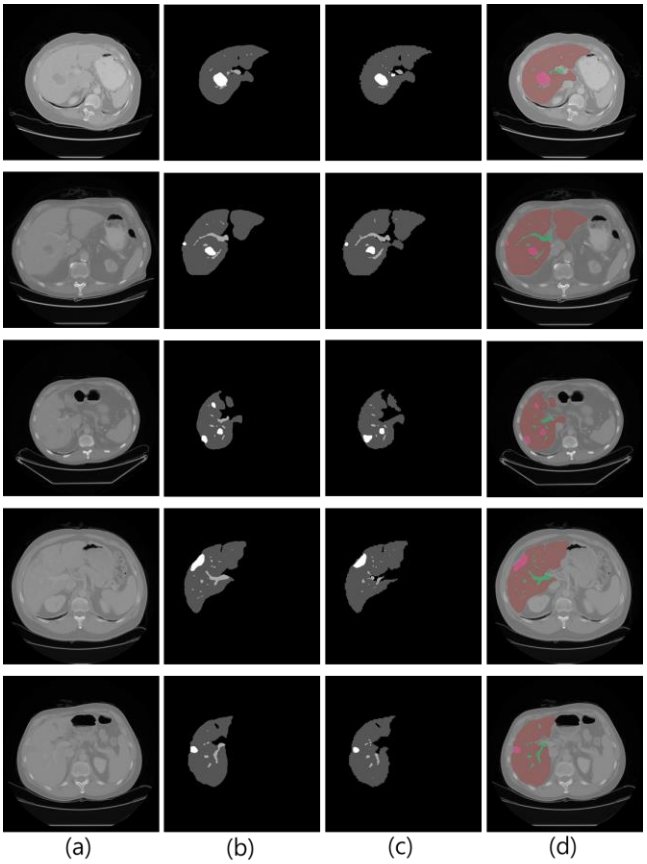

Figure 7: Segmentation result: (a)original CT image, (b)segmented result, (c)original ground truths, (d) overlay image.

3.2 Quantitative Evaluation

Quantitative evaluation is conducted through two primary methods: assessing the performance of the segmentation model

and comparing its results with the actual staging. First, the performance of the segmentation model is evaluated using ground truth (GT) images provided by Decathlon and the resulting segmentation outcomes. Accuracy is calculated to measure the model's overall precision. Accuracy represents the ratio of correctly predicted data points to the total number of data points.

$$Accuracy = \frac{TP + TN}{TP + TN + FP + FN} \quad (3)$$

TP(True Positive) denotes cases where the model correctly predicts a positive outcome, TN(True Negative) indicates cases where the model correctly predicts a negative outcome, FP(False Positive) refers to cases where the model incorrectly predicts a positive outcome, and FN(False Negative) indicates cases where the model incorrectly predicts a negative outcome. A higher accuracy value, closer to 1, indicates greater precision.

Next, the Dice Similarity Coefficient (DSC) is used to measure the overlap between the predicted segmentation and the GT. A represents the predicted segmentation, B represents the GT, and $|A \cap B|$ denotes the size of the intersection between the two regions. A DSC value closer to 1 indicates higher similarity between the two sets.

$$DSC = \frac{2 \times |A \cap B|}{|A| + |B|} \quad (4)$$

Finally, the Volumetric Overlap Error (VOE) is employed to measure the portion of the segmented region that does not overlap with the actual region. In this case, A denotes the predicted segmentation, B denotes the GT, $|A \cap B|$ represents the size of the intersection between the two regions, and $|A \cup B|$ indicates the size of the union of the two regions. A smaller VOE value signifies better segmentation performance.

$$P = P_1 + \frac{v_t - v_1}{v_2 - v_1}(P_2 - P_1) \quad (5)$$

Table 2: Segmentation Model Results

	Accuracy (%)	DSC (%)	VOE (%)
Liver	95.09	95.04	9.42
Liver vessel	81.16	73.02	36.97
Liver tumor	87.97	81.73	27.45

The performance of the segmentation model was evaluated using these three metrics, with the results shown in Table 2. Metrics were calculated for each label liver, liver vessels, and liver tumors. The average Accuracy for these labels was 88.07%, the Dice Similarity Coefficient was 83.274%, and the Volumetric Overlap Error was 24.61%, indicating effective segmentation.

Table 3: Accuracy Evaluation

		Predicted			
		Stage 1	Stage 2	Stage 3	Stage 4
Actual	Stage 1	4	1	1	0
	Stage 2	0	4	0	0
	Stage 3	0	0	5	0
	Stage 4	0	0	1	4

Subsequently, the accuracy of the proposed staging method is evaluated by comparing it with the actual staging diagnosed by clinicians. Table 3 shows the accuracy assessment results for 20 cases of hepatocellular carcinoma patients, demonstrating a high accuracy of 85%.

4 CONCLUSIONS

In this paper, we proposed an automatic method for liver tumor segmentation and staging. The proposed method segments the liver, liver vessels, and liver tumors regions from abdominal CT images of hepatocellular carcinoma patients. It then generates surface meshes from the segmented regions and determines the staging based on tumor diameter, number, and vascular invasion using the generated surface meshes. The performance of both the segmentation and staging methods was evaluated through experiments. The results showed that the segmentation model achieved an accuracy of 88.07%, a Dice Similarity Coefficient of 83.27%, and a Volumetric Overlap Error of 24.61%, while the staging accuracy reached 85%, demonstrating the high effectiveness of the proposed method.

These results demonstrate that the proposed method can reduce the need for physicians to manually compare and review numerous CT images, serving as a rapid, objective, and accurate diagnostic aid. Furthermore, future research will focus to enhance the proposed method by incorporating the analysis of metastasis and blood test results, with the goal of developing a more precise staging technique. Additionally, the proposed method will be applied in clinical settings to validate its effectiveness and assess its performance across various clinical scenarios. The ultimate goal is to develop the proposed method into a practical diagnostic tool for liver cancer diagnosis and staging.

ACKNOWLEDGMENTS

This work was partly supported by the National Research Foundation of Korea(NRF) grant funded by the Korea government(MSIT) (No. 2020R1A2C1102727). And this research was partly supported by Basic Science Research Program through the National Research Foundation of Korea (NRF) funded by the Ministry of Education (grant number: RS-2023-00244520)

REFERENCES

[1] H. Sung, J. Ferlay, R. L. Siegel, M. Laversanne, I. Soerjomataram, A. Jemal, and F. Bray. 2021. Global Cancer Statistics 2020: GLOBOCAN Estimates of Incidence and Mortality Worldwide for 36 Cancers in 185 Countries. CA: A Cancer Journal for Clinicians 71, 3 (2021), 209-249. DOI:https://doi.org/10.3322/caac.21660

[2] D. Suresh, A. N. Srinivas, A. Prashant, K. B. Harikumar, and D. P. Kumar. 2023. Therapeutic options in hepatocellular carcinoma: a comprehensive review. Clinical and Experimental Medicine 23, 6 (2023), 1901-1916. DOI:https://doi.org/10.1007/s10238-023-01014-3

[3] J. M. Llovet, R. K. Kelley, A. Villanueva, A. G. Singal, E. Pikarsky, S. Roayaie, R. Lencioni, K. Koike, J. Zucman-Rossi, and R. S. Finn. 2021. Hepatocellular carcinoma. Nature Reviews Disease Primers 7, 1 (2021). DOI:https://doi.org/10.1038/s41572-020-00240-3

[4] K. O. Asafo-Agyei, and H. Samant. 2023. Hepatocellular Carcinoma. StatPearls, StatPearls Publishing (2023). PMID: 32644603.

[5] R.V. Manjunath and K. Kwadiki. 2022. Automatic liver and tumour segmentation from CT images using Deep learning algorithm. Results in Control and Optimization 6, (2022), 100087. DOI:https://doi.org/10.1016/j.rico.2021.100087

[6] V. R. Kavitha, F. B. J. Hussain, P. Chillakuru, and P. Shanmugam. 2024. Automated Classification of Liver Cancer Stages Using Deep Learning on Histopathological Images. Traitement du Signal 41, 1 (2024), 373-381. DOI:https://doi.org/10.18280/ts.410131

[7] Y. Xu, C. Zhou, X. He, R. Song, Y. Liu, H. Zhang, Y. Wang, Q. Fan, W. Chen, J. Wu, J. Wang, and D. Guo. 2023. Deep learning–assisted LI-RADS grading and distinguishing hepatocellular carcinoma (HCC) from non-HCC based on multiphase CT: a two-center study. European Radiology 33, 12 (2023), 8879-8888. DOI:https://doi.org/10.1007/s00330-023-09857-w

[8] A. Midya, J. Chakraborty, R. Srouji, R. R. Narayan, T. Boerner, J. Zheng, L. M. Pak, J. M. Creasy, L. A. Escobar, K. A. Harrington, M. Gönen, M. I. D'Angelica, T. P. Kingham, R. K. G. Do, W. R. Jarnagin, and A. L. Simpson. 2023. Computerized Diagnosis of Liver Tumors From CT Scans Using a Deep Neural Network Approach. IEEE Journal of Biomedical and Health Informatics 27, 5 (2023), 2456-2464. DOI:https://doi.org/10.1109/jbhi.2023.3248489

[9] Ö. Çiçek, A. Abdulkadir, S. S. Lienkamp, T. Brox, and O. Ronneberger. 2016. 3D U-Net: Learning Dense Volumetric Segmentation from Sparse Annotation. Medical Image Computing and Computer-Assisted Intervention – MICCAI 2016 (2016), 424-432. DOI:https://doi.org/10.1007/978-3-319-46723-8_49

[10] M. Antonelli, A. Reinke, S. Bakas, K. Farahani, A. Kopp-Schneider, B. A. Landman, G. Litjens, B. Menze, O. Ronneberger, R. M. Summers, B. V. Ginneken, M. Bilello, P. Bilic, P. F. Christ, R. K. G. Do, M. J. Gollub, S. H. Heckers, H. Huisman, W. R. Jarnagin, M. K. McHugo, S. Napel, J. S. G. Pernicka, K. Rhode, C. Tobon-Gomez, E. Vorontsov, J. A. Meakin, S. Ourselin, M. Wiesenfarth, P. Arbeláez, B. Bae, S. Chen, L. Daza, J. Feng, B. He, F. Isensee, Y. Ji, F. Jia, I. Kim, K. Maier-Hein, D. Merhof, A. Pai, B. Park, M. Perslev, R. Rezaiifar, O. Rippel, I. Sarasua, W. Shen, J. Son, C. Wachinger, L. Wang, Y. Wang, Y. Xia, D. Xu, Z. Xu, Y. Zheng, A. L. Simpson, L. Maier-Hein, and M. J. Cardoso. 2022. The Medical Segmentation Decathlon. Nature Communications 13, 1 (2022). DOI:https://doi.org/10.1038/s41467-022-30695-9

[11] A. W. Moawad, D. Fuentes, A. Morshid, A. M. Khalaf, M. M. Elmohr, A. Abusaif, J. D. Hazle, A. O. Kaseb, M. Hassan, A. Mahvash, J. Szklaruk, A. Qayyom, and K. Elsayes. 2021. Multimodality annotated HCC cases with and without advanced imaging segmentation [Data set]. The Cancer Imaging Archive (2021). DOI:https://doi.org/10.7937/TCIA.5FNA-0924

[12] J. Wasserthal, H. Breit, M. T. Meyer, M. Pradella, D. Hinck, A. W. Sauter, T. Heye, D. T. Boll, J. Cyriac, S. Yang, M. Bach, and M. Segeroth. 2023. TotalSegmentator: Robust Segmentation of 104 Anatomic Structures in CT Images. *Radiology: Artificial Intelligence* 5, 5 (2023). DOI:https://doi.org/10.1148/ryai.230024

[13] F. Isensee, P. F. Jaeger, S. A. A. Kohl, J. Petersen, and K. H. Maier-Hein. 2020. nnU-Net: a self-configuring method for deep learning-based biomedical image segmentation. *Nature Methods* 18, 2 (2020), 203-211. DOI:https://doi.org/10.1038/s41592-020-01008-z

[14] P. Perona and J. Malik. 1990. Scale-space and edge detection using anisotropic diffusion. IEEE Transactions on Pattern Analysis and Machine Intelligence 12, 7 (1990), 629-639. DOI:https://doi.org/10.1109/34.56205

[15] W. Schroeder, R. Maynard, and B. Geveci. 2015. Flying edges: A high-performance scalable isocontouring algorithm. 2015 IEEE 5th Symposium on Large Data Analysis and Visualization (LDAV) (2015). DOI:https://doi.org/10.1109/ldav.2015.7348069

[16] M. B. Amin, F. L. Greene, S. B. Edge, C. C. Compton, J. E. Gershenwald, R. K. Brookland, L. Meyer, D. M. Gress, D. R. Byrd, and D. P. Winchester. 2017. The Eighth Edition AJCC Cancer Staging Manual: Continuing to build a bridge from a population-based to a more "personalized" approach to cancer staging. CA: A Cancer Journal for Clinicians 67, 2 (2017), 93-99. DOI:https://doi.org/10.3322/caac.21388